Environmental Pollution 373 (2025) 126135

Contents lists available at ScienceDirect

Environmental Pollution

journal homepage: www.elsevier.com/locate/envpol

Comparative secretome and proteome analysis unveils the response mechanism in the phosphorus utilization of *Alexandrium pacificum*☆

Xiaohang Li [a,c,1], Xi Chen [b,1], Shuxue Zhao [a,e], Hua Jiang [a,c], Yuqin Cai [a,c], Jie Bai [a,c], Jiajun Shao [d], Hao Yu [d,*], Tiantian Chen [a,c,**]

[a] College of Environmental Science and Engineering, Ocean University of China, Qingdao, 266100, China
[b] College of Marine Life Sciences, Ocean University of China, Qingdao, 266003, China
[c] Key Laboratory of Marine Environment and Ecology, Ocean University of China, Qingdao, 266100, China
[d] Shandong Provincial Key Laboratory of Applied Mycology, School of Life Sciences, Qingdao Agricultural University, Qingdao, 266109, Shandong Province, China
[e] Shandong Key Laboratory of Edible Mushroom Technology, Yantai Edible and Medicinal Mushroom Technology Innovation Center, School of Horticulture, Ludong University, Yantai, 264025, China

ARTICLE INFO

Keywords:
Alexandrium pacificum
Phosphorus
Alkaline phosphatase
Comparative proteome
Comparative secretome
Molecular response

ABSTRACT

Phosphorus (P) acts as a crucial limiting nutrient for the growth of marine phytoplankton cells and the formation of algal blooms. The dinoflagellate *Alexandrium pacificum* is known for causing frequent and intense blooms in specific estuarine and coastal regions. In this study, we investigated the growth and physiological transformations under conditions characterized by P-deficiency, NaH_2PO_4, and ATP. For the first time, an integrated comparative analysis of the secretome and proteome was performed to investigate the global protein expression profile of *A. pacificum*, with 355 and 2308 differentially expressed proteins (DEPs), respectively. The results demonstrated that P-deficiency led to a reduction in growth and notable decreases in metabolic processes in *A. pacificum*. In P-deficient and ATP groups, the expression of secretory protein alkaline phosphatase A (PhoA) was increased, while intracellular acid phosphatase (ACP) displayed significant upregulation in P-deficient group, indicating that *A. pacificum* has evolved multiple organic P utilization strategies to adapt to low-P environments. *A. pacificum* can utilize the intracellular carbohydrate storage pools via glycolysis and the TCA cycle to replenish Calvin cycle intermediates. However, the growth of the ATP and NaH_2PO_4 groups showed no significant alteration. These results suggest that *A. pacificum* possesses distinct adaptive strategies towards P-deficiency in the environment and employs specific mechanisms for utilizing organic P, which may be a crucial factor in the formation of blooms in low inorganic P environments.

1. Introduction

In recent decades, the frequency and scale of global extensive blooms have been increasing continuously, emerging as a significant marine calamity of global concern (Smayda, 2001). Dinoflagellates, as one of the primary biological communities of harmful algal blooms (HABs) (Wang et al., 2014; Lin et al., 2015; Gong et al., 2017), profoundly disrupt the marine ecological environment and significantly impact the economic benefits of aquaculture (Anderson et al., 1990; Hallegraeff, 2003). Certain toxic phytoplankton can produce harmful metabolites, further raising concerns about the impact on human health (Zhang et al., 2019a; Leal and Cristiano, 2022). The increased occurrence frequency of blooms is primarily associated with environmental and climatic changes, as well as eutrophication (Leal and Cristiano, 2022). Nutrients are considered a key factor, with P being a crucial determinant of algal abundance (Paerl et al., 2011; Paerl and Otten, 2013; Zhang et al., 2021).

Phosphorus is crucial in sustaining life, serving as a vital constituent of biological molecules such as DNA, RNA, ATP, phospholipids, and signaling molecules, and is essential for the growth of phytoplankton

☆ This paper has been recommended for acceptance by Charles Wong.

* Corresponding author. Shandong Provincial Key Laboratory of Applied Mycology, School of Life Sciences, Qingdao Agricultural University, Qingdao, 266109, Shandong Province, China.
** Corresponding author. College of Environmental Science and Engineering, Ocean University of China, Qingdao, 266100, China.
E-mail addresses: yuhaosunshine@163.com (H. Yu), chentiantian@ouc.edu.cn (T. Chen).

[1] These authors contributed equally to this work.

https://doi.org/10.1016/j.envpol.2025.126135
Received 18 November 2024; Received in revised form 13 March 2025; Accepted 25 March 2025
Available online 26 March 2025

(Karl, 2000; Dyhrman, 2016; Lin et al., 2016). The acquisition of P from marine dissolution primarily stems from the gradual process of rock weathering, distinguishing it from nitrogen (Tyrrell, 1999; Laakso et al., 2020), thus its concentration in the surface waters of open oceans is extremely low. Additionally, due to anthropogenic nitrogen overload, coastal waters are often under P limitation (Lin et al., 2016). Therefore, the growth of marine phytoplankton and primary productivity are predominantly constrained by P (Thingstad et al., 2005; Schindler et al., 2008). The P in the dissolved state primarily exists in two forms: inorganic P and organic P (Orchard et al., 2009). Dissolved inorganic P (DIP) mainly exists in the form of orthophosphate ions (Luo et al., 2017), which can be directly absorbed by phytoplankton. Dissolved organic P (DOP) is not directly utilized by phytoplankton (Casey et al., 2009), but dinoflagellates are capable of maintaining their cellular growth by utilizing DOP when DIP is insufficient (Dyhrman, 2016; Lin et al., 2016), and this ability has become a potential competitive advantage for these species in phytoplankton competition (Chen et al., 2024). Transcriptomic analysis revealed that *Prorocentrum shikokuense* can cope with P-deficiency through membrane phospholipid restructuring and autophagy (Li et al., 2024). The coordinated synthesis and degradation of polyphosphate play a crucial role in maintaining P homeostasis in *Karenia mikimotoi* (Jin et al., 2023). While researchers report that alkaline phosphatase can hydrolyze DOP for utilization, the absorption and response mechanisms of dinoflagellates to P variations in the environment are still not very clear at present (Dyhrman et al., 2007; Zhang et al., 2017, 2019b).

Alexandrium pacificum is a prevalent toxic and harmful dinoflagellate, capable of generating paralytic shellfish toxins (PSTs) (Penna et al., 2005). Initially, it was detected in the coastal waters of many Mediterranean countries and subsequently considered to be an introduced alien species due to human activities (Wyatt and Jenkinson, 1997; Lilly, 2002). In recent years, due to high nitrogen and low P loading, the Yangtze River Estuary and its adjacent East China Sea have become one of the most severely eutrophic and P-deficient areas in China. However, as a region where large-scale Pacific algal blooms frequently occur (Zhou et al., 2008; Yu et al., 2017), it is accompanied by high chlorophyll *a* concentrations and simultaneously high DOP concentrations (Huang et al., 2007; Chen et al., 2024). Studies indicate that *A. pacificum* possesses the capability to utilize a variety of DOP, such as adenosine 5-triphosphate (ATP), D-glucose 6-phosphate (G-6-P), and β-glycerol phosphate (SG-P), by regulating growth, photosynthesis, and the synthesis of gene clusters in response to environmental changes (Van Mooy et al., 2009; Chen et al., 2024). However, in comparison to other phytoplankton, the investigation into the molecular regulatory mechanisms underlying the response of *A. pacificum* to environmental phosphate fluctuations, particularly concerning P-deficiency and ample DOP supply, remains significantly limited. This impetus drives us towards a deeper comprehension of the physiological responses and potential molecular pathways implicated in the environmental phosphate variations of *A. pacificum*.

In this study, we used *A. pacificum* collected from the Yangtze River estuary adjacent waters as our materials. We conducted a comparative proteome analysis and combined it with the secretome to evaluate the protein expression profiles of *A. pacificum* under P-deficient, DIP-replete (NaH_2PO_4), and DOP-replete (ATP) conditions. Integrated with physiological and biochemical response parameters, we characterized DEPs and further investigated the molecular mechanisms related to growth, photosynthesis, and toxin synthesis. This study will contribute to a better comprehension of the adaptive strategies and response mechanisms of *A. pacificum* to P variations, providing a basis for its frequent blooms in the Yangtze River Estuary and its adjacent sea areas.

2. Materials and methods

2.1. Strain and culture conditions

The *A. pacificum* algae strain in this study was isolated in the earlier stages from the laboratory (Chen et al., 2024). The strain was inoculated into a f/2 medium lacking $Na_2SiO_3 \bullet 9H_2O$ (f/2-Si) (Huang et al., 2024; Li et al., 2024) prepared with natural seawater (salinity of 30 ± 0.1) filtered through a 0.22 μm membrane and sterilized under high pressure, and cultivated under conditions of 20 ± 1 °C, 75 μE m^{-2} s^{-1} under a 12 h:12 h light: dark cycle of white fluorescent light (Guillard and Ryther, 1962). The axenic stock cultures were regularly transferred to fresh f/2-Si culture medium to sustain it in the exponential growth phase. Before the experiment, the strains were pre-cultured under P-deficient f/2-Si medium for 48 h to exhaust intracellular phosphate reserves through starvation cultivation.

2.2. Growth rate and cell morphological changes of A. pacificum

The strain of *A. pacificum* was cultured in f/2-Si medium with 36 μmol P L^{-1} of NaH_2PO_4 and ATP as the sole P source or P-deficient conditions. The initial cell density in the experimental group was 200 ± 10 cells mL^{-1}, under identical conditions, the cultures were maintained for 14 days in triplicates. Algal cell counts were performed every other day using an inverted microscope (IX71, Olympus, Japan).

By collecting equal aliquots of algal culture medium from both P-deficient condition (0 μmol P L^{-1}) and P-replete conditions (containing 36 μmol P L^{-1} as NaH_2PO_4 and ATP), which were cultivated up to the 6th and 10th days respectively, the samples were then fixed overnight in a solution of 2.5 % glutaraldehyde at a temperature of 4 °C. An upright fluorescence microscope was used for capturing images, and the captured images were analyzed using Image J software yielding the equivalent spherical diameter (ESD) and MinFeret diameter of the microalgae. Furthermore, cell volume (*V*) and surface area (*S*) were calculated using the following formulas:

$$V = \frac{4}{3} A \sqrt{\frac{dA}{\pi l}} \tag{1}$$

$$S = \pi d\, l \tag{2}$$

where A represented the measurement of the area, d represented the minimum Feret diameter, and l represented the Feret diameter (Ge et al., 2022).

2.3. P concentration and alkaline phosphatase activity

Water samples intended for the analysis of inorganic and organic P content are filtered through a Whatman GF/F filter (0.7 μm pore size, 25 mm in diameter, Whatman Inc.) using a vacuum pump (<0.02 MPa), retaining the supernatant. Subsequently, the concentration of DIP is determined through the molybdenum blue method, while total dissolved P (TDP) and DOP are measured following the method reported by Jeffries et al. (1979). The simultaneous acquisition of an additional 20 mL aliquot of medium for gentle centrifugal enrichment (4°C, 2000× g, 10 min) led to the measurement of alkaline phosphatase activity (APA), as described previously (Lin et al., 2012b).

2.4. Chl a content and photosynthesis activity

10 mL of the medium were filtered through a 25 mm GF/F glass microfiber filter (Whatman, USA), the filter was submerged in a 90 % acetone solution for an overnight extraction under dark conditions at 4 °C and quantified using the Trilogy Laboratory Fluorometer (Turner Designs Inc.). The Chl a content was calculated using the method described previously (Parsons et al., 1984).

Photochemical efficiency was measured using a pulse-amplitude-modulated fluorometer (PhytoPAM II Walz, Effeltrich, Germany). Among these, F_v/F_m represents the photochemical efficiency of the PS II reaction center, indicating the quantum yield when the PS II is fully open. F_v/F_0 signifies the potential photosynthesis activity of PS II, and F_v'/F_m' denotes the effective quantum yield of the PS II reaction center, which is calculated using the following formula:

$$\frac{F_v}{F_m}=\frac{F_m-F_0}{F_m} \tag{3}$$

$$\frac{F_v}{F_0}=\frac{F_m-F_0}{F_0} \tag{4}$$

$$\frac{F_v'}{F_m'}=\frac{F_m'-F_0'}{F_m'} \tag{5}$$

where F_v represented variable fluorescence, F_m represented maximum fluorescence, F_0 represented minimum fluorescence, F_m' represented actual maximum fluorescence, and F_0' represented actual minimum fluorescence, respectively. The sample underwent a dark adaptation of 15 min before the measurement.

A rapid light-response curve (RLC) was generated with an illumination duration of 20 s, encompassing 12 light intensity points from 9 to 2293 μmol m^{-2} s^{-1}. The initial slope of the photosynthesis efficiency (α), maximum photosynthesis rate at maximum electron transfer efficiency (*rETRmax*), and half-saturation light intensity (I_k) indicating the capability to adapt to light intensity were all recorded (Ralph and Gademann, 2005; Houliez et al., 2017).

2.5. Proteins sequencing and bioinformatics analysis

Algal cells of *A. pacificum* were cultivated for 10 days, and the supernatant of the medium collected after 6 and 10 days was used for protein extraction. The medium was centrifuged at 4000×*g* for 10 min at 4 °C. The supernatant was filtered through a 0.22 μm membrane (Yegorov et al., 2021), and secreted proteins were extracted using the phenol method (Zhao et al., 2024). Briefly, 30 mL of supernatant was collected, mixed with 10 mL of Tris-saturated phenol (TS-Phe; Solarbio, Beijing, China), and centrifugated at 8000×*g* for 10 min. The supernatant was combined with an equal volume of phenol extraction buffer (0.7 M sucrose; 0.1 M KCl; 0.5 M Tris-HCl, pH 7.5; 50 mM EDTA), thoroughly mixed, and centrifuged at 10,000×*g* for 10 min. The aqueous phase was transferred, and proteins were precipitated by adding five volumes of 0.1 M ammonium acetate (AAM), followed by overnight incubation at −20 °C. Precipitated proteins were collected by centrifugation at 10,000×*g* for 10 min, washed twice with methanol and acetone, respectively, and dissolved in 300 μL of UT Buffer (8 M urea; 0.1 M Tris-HCl, pH 8.5). Protein concentration was determined using the BCA assay.

For intracellular protein extraction (Xu et al., 2023), algal cells were washed with sterile seawater, snap-frozen in liquid nitrogen, and stored at −80 °C. Frozen cells were resuspended in 1 mL of UT buffer supplemented with Halt Protease Inhibitor Cocktail (Thermo Fisher Scientific, Shanghai, China), disrupted using a TissueLyser II system (QIAGEN, Hilden, Germany) at 150 Hz for 1 min, and sonicated for 24 s (6 s on, 15 s off). Cellular debris was removed by centrifugation at 12,000×*g* for 10 min at 4 °C, and protein concentration in the clarified supernatant was quantified by BCA assay. Peptide digestion and bioinformatics analysis for secretory and intracellular proteins are detailed in the Supplementary Materials.

3. Results

3.1. Physiological responses of A. pacificum various P compounds

P-deficient (NP) treatment exhibited complete growth arrest, with cell densities consistently below 0.36 ± 0.01 × 10^3 cells mL^{-1} (Fig. 1A). In contrast, P-replete groups sustained active proliferation until the experimental endpoint. No significant difference ($p > 0.05$) was observed in final cell densities between the NaH_2PO_4 (IP) (32.71 ± 0.15 × 10^3 cells mL^{-1}) and ATP (32.41 ± 1.53 × 10^3 cells mL^{-1}) treatments. Concomitant with the growth patterns, distinct phosphorus utilization dynamics were observed (Fig. 1B and C). In the IP treatment, dissolved inorganic phosphorus (DIP) decreased from 36 μmol L^{-1} to 2.27 ± 0.13 μmol L^{-1} by day 6, while the ATP group exhibited a similar depletion of dissolved organic phosphorus (DOP) to 2.63 ± 0.17 μmol L^{-1}. Notably, DIP accumulation peaked at 26.74 ± 0.15 μmol L^{-1} on day 6 under ATP treatment, followed by gradual depletion over the subsequent 6-day period.

Significant expressions of APA were found in P-deficient group (Fig. 1D and E), reaching maximum values of 29.97 ± 1.61 fmol $cell^{-1}$ h^{-1} (intracellular) and 0.11 ± 0.01 μmol L^{-1} h^{-1} (extracellular). In contrast, P-replete groups exhibited a gradual increase, with a significant difference ($P < 0.05$) between ATP (0.12 ± 0.01 μmol L^{-1} h^{-1}) and IP (0.08 ± 0.01 μmol L^{-1} h^{-1}) group.

The survival of marine microalgae under abiotic/biotic stressors is significantly influenced by the process of photosynthesis. While chlorophyll *a* content gradually declined, and there were no significant differences ($P > 0.05$) among the three groups after 6 days (Fig. 1F). The F_v/F_m values of P-replete groups fluctuated between 0.24 and 0.49 throughout the experiment (Fig. 1G), and P-deficient culture maintained below 0.16. F_v'/F_m' and F_v/F_0 exhibited similar trends, revealing a significant difference observed between P-deficient and P-replete groups ($P < 0.01$). After 48 h of cultivation, Fig. 1H indicates a significant reduction in RLC in P-deficient group ($P < 0.01$), while no significant difference was observed between P-replete groups ($P > 0.05$). Additionally, at 6 days, both I_k and *rETRmax* reached peak values, with the IP group being 1.25 times and 1.12 times greater than those in the ATP culture, respectively.

P-deficiency resulted in a substantial augmentation of cell size, *S* and *V* of P-deficient group exhibited an increase of 90.89–114.09 % and 255.23–283.09 %, respectively (Fig. S1A). In contrast, The ESD measurements of the IP group predominantly fell within the intervals of 21–23 μm (6 days) and 24–26 μm (10 days), whereas the ATP group consistently maintained ESD values within the range of 23–25 μm (Fig. 1I).

3.2. Secretome profile of A. pacificum under various P compounds

A label-free quantitative proteomic approach was performed to analyze the secretome of *A. pacificum* with different groups. A total of 447 proteins were identified in the secretome, only 7 proteins (1.6 %) detected in all experimental cultures (Fig. 2A). Principal Coordinate Analysis (PCoA) revealed that P is responsible for 44.89 % of PCoA1 level for the secretome of *A. pacificum* (Fig. 2B), and horizontal disparities were observed between P-deficient and P-replete groups. As shown in Fig. 2C, the within-group correlation on the tenth day (TN, TD, TA) surpasses that of the sixth day (XN, XD, XA).

Proteins with $|\log_2(\text{fold change})| > 0.585$ and a false discovery rate (FDR) < 0.05, or unique proteins reaching 70 % expression in one group compared to other groups are identified as differentially expressed proteins (DEPs). Comparing TD with TN exhibited the highest number of DEPs among all comparison groups (totaling 268, with 92.5 % uniDEPs) (Fig. S2A, Table S1). Through the integration of DEPs from comparative analyses using Venn diagrams, 19 and 50 uniDEPs were identified respectively (Fig. 2D–Table S2), with a heatmap depicting the expression of 69 uniDEPs at different stages (Figs. S2B and C), signifying a significant alteration in the *A. pacificum* secretion spectrum as cultivation time progresses. The TD group exhibits the highest relative abundance of secretory proteins (Fig. S1B), within the TD vs. TN comparison, secretory proteins account for 19.81 % of upregulated DEPs. Conversely, downregulated DEPs primarily consist of secretory proteins within the

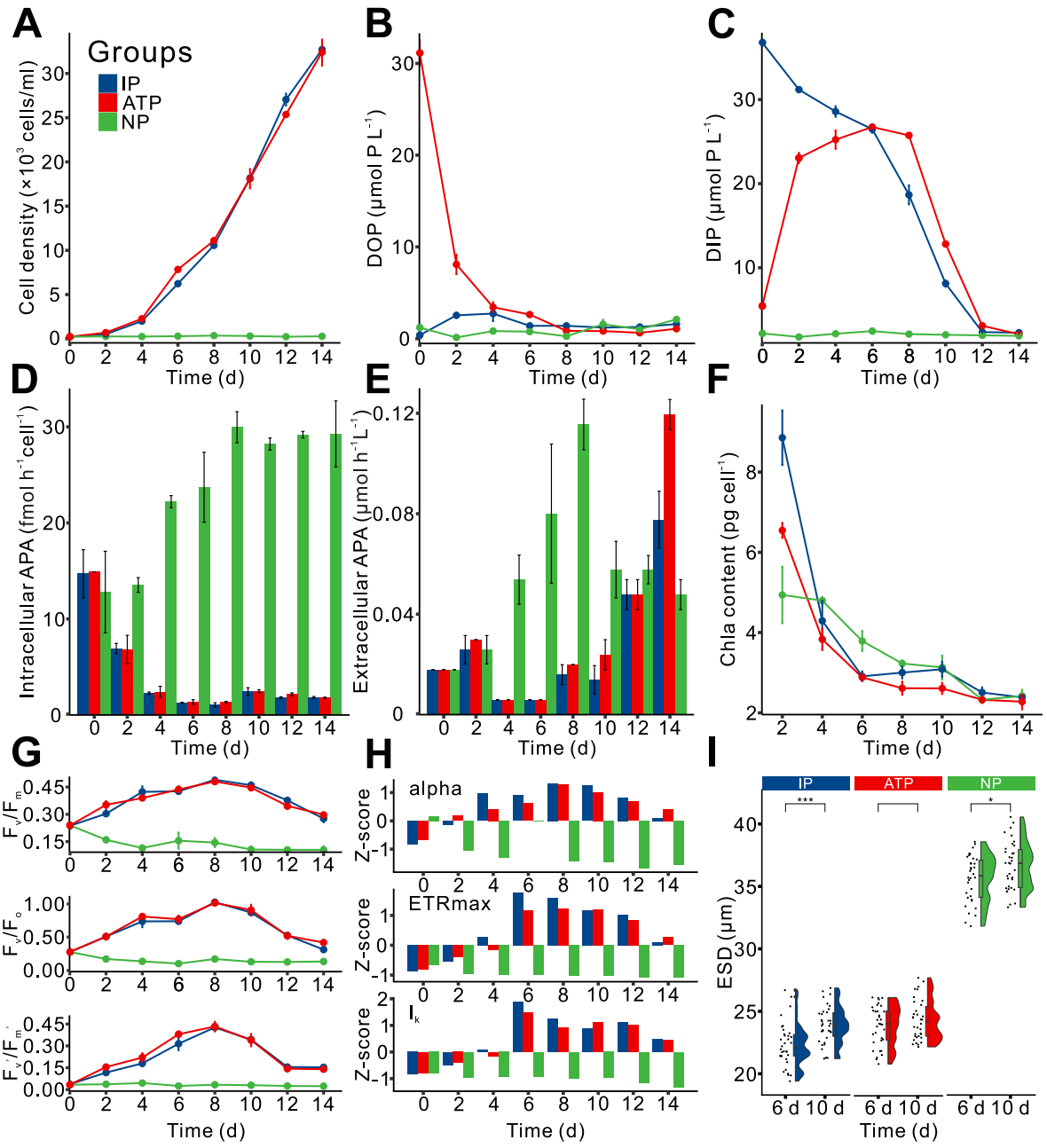

Fig. 1. Physiological and biochemical responses of *A. pacificum* to various P. (A) Cell density, (B) DOP concentration, (C) DIP concentration, (D) Intracellular APA, (E) Extracellular APA, (F) Chl a content, (G) Photosynthetic efficiency, (H) Rapid light-response curve parameters, (I) Equivalent spherical diameter.

TA vs TD comparison. Moreover, TN and XN groups show a higher ratio of secretory proteins, but the lower number in DEPs (Fig. 2E, Fig. S1C). The MW of secretory proteins associated with upregulated DEPs demonstrated distinct patterns across TD vs. TN and TA vs. TD comparisons, suggesting that both P-deficient and ATP groups demonstrate a tendency to express secretory proteins with relatively smaller molecular weights (Fig. 2E–Table S3).

Those secretory protein led to its division into eight categories (Fig. S2D). High abundance of phosphatases was observed in the XN group, and the XA group exhibited a notably higher concentration of proteases, hydrolases, transferases, and lipases, alongside a reduction of other functional proteins. The presence of restricted but noticeable phosphatases was detected in the XA group, including a 4.92-fold upregulation of PhoA compared with IP group and low-abundance alkaline phosphatase D (PhoD) expression, suggesting that ATP utilization by *A. pacificum* may involve both hydrolysis and direct uptake processes (Luo et al., 2017; Chen et al., 2024). The TN group demonstrated an increase in both the expression of phosphatase and lipase enzymes. Previous research suggests that a lack of P leads to reduced phospholipid synthesis while boosting lipid metabolic efficiency (Li et al., 2024) (Fig. 2F, Fig. S2D, Table S3). The expression of peptidases and hydrolases such as serine protease (TRINITY_DN5314_c0_g2_i3.p1), PhoD (TRINITY_DN14438_c0_g1_i2.p1), Pectin acetylesterase (Pat) (TRINITY_DN841_c0_g1_i2.p1) and Dienelactone hydrolase (DlH) (TRINITY_DN4738_c0_g2_i4.p1) was significantly upregulated in P-replete groups (Fig. 2G and Table S3). Conversely, other type proteins were upregulated in P-deficient group, and the expression of peptidase S8 (TRINITY_DN4374_c0_g2_i1.p1) was upregulated on day 10. The S8 family represents a broadly classified group of peptidases, whose members share a conserved catalytic triad (Asp, His, and Ser). This upregulation might be associated with P-deficiency-induced cell growth arrest (Levin et al., 2019).

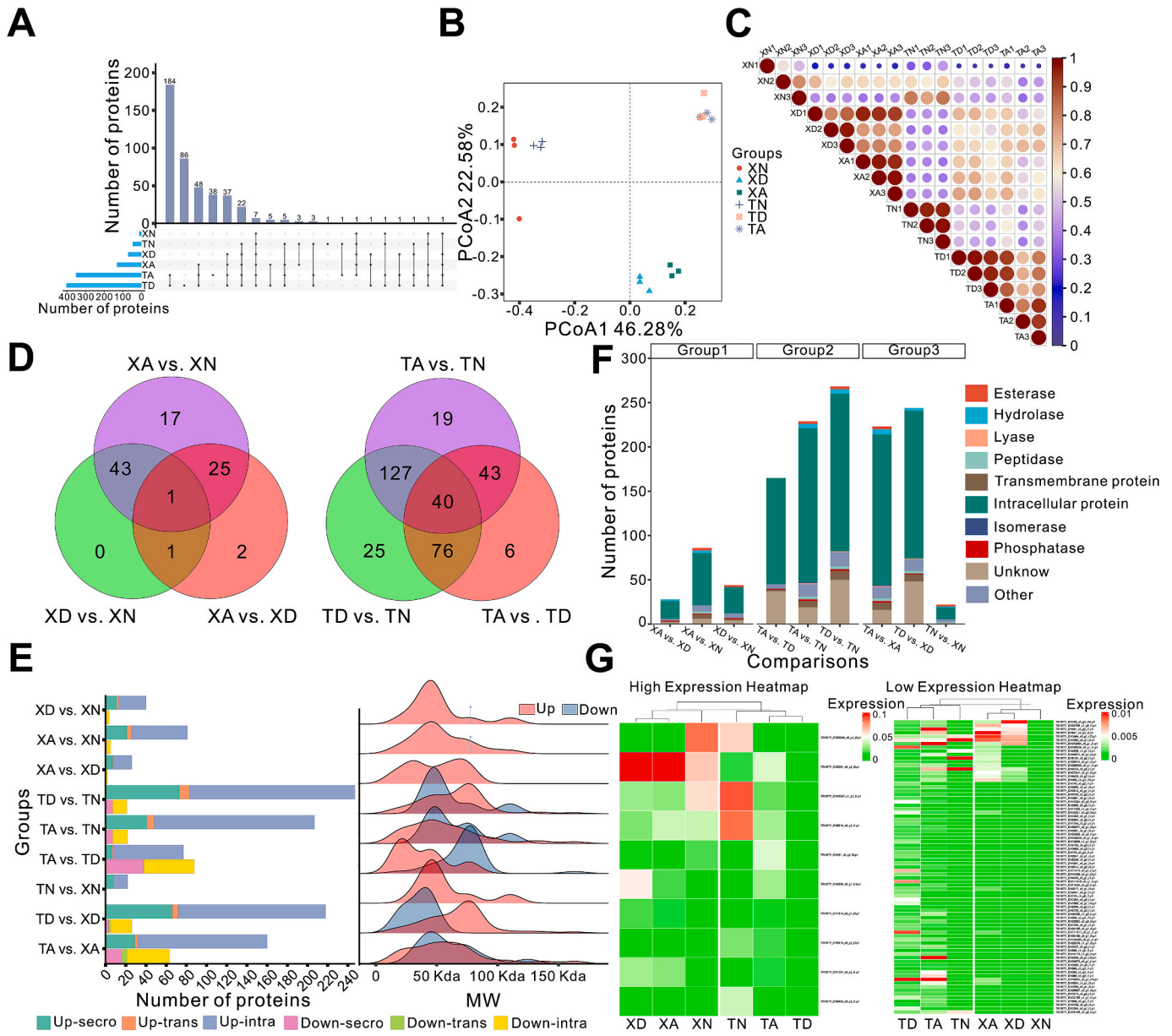

Fig. 2. Statistics analysis of the secretome data of *A. pacificum* samples under various P conditions. (A) Upset diagram demonstrating the number of expressed proteins. PCoA (B) and PCC (C) analysis of *A. pacificum* growing on different P mediums for 6 and 10 days. (D) Venn diagrams of the intersection and the number of all nonredundant DEPs among three comparisons from the 6 and 10 days, respectively. (E) Proteins classification of comparisons and statistics of the upregulated and downregulated DEPs with molecular weight distribution of secreted proteins. (F) DEPs across comparative groups were functionally categorized into ten distinct classes based on their biological functions. (G) The different expression of high and low abundance secreted proteins in various treatments.

3.3. *Proteome profile of A. pacificum under various P compounds*

A total of 3942 quantifiable proteins were identified, with 1669 proteins (42.34 %) detected in all three groups (Fig. 3A and Table S4). Principal Component Analysis (PCA) results revealed distinct clustering of samples across different groups (Fig. 3B). Samples from the P-depleted group are situated in the left quadrant, demonstrating a strong alignment between protein expression patterns and analytical outcomes. Between the IP and ATP groups, correlations above 0.97 were observed, contrasting with a slightly lower correlation within the NP group below 0.95 (Fig. 3C). Furthermore, the NP group is characterized by a higher proportion of secreted proteins (Figs. S1D and S1E), showing lower correlations with transmembrane and intracellular proteins, relative to secreted proteins (Fig. 3C).

A total of 2,090, 2,022, and 130 DEPs were selected in all three groups (Fig. 3D and Table S5). The proportion of downregulated proteins in P-replete groups is higher for secreted and transmembrane proteins (Fig. S3A). The subcellular localization of DEPs reveals predominant distribution across mitochondria, cytoplasm, extracellular space, and nucleus (Fig. 3E). The molecular weights of distinct proteins cluster primarily within the 9.61–101.87 kDa range. Isoelectric points (pI) predominantly fall within 3.78–11.61. Moreover, the GRAVY values for these proteins are confined to the interval from −0.97 to 0.44. The median molecular weight of ATP vs. IP upregulated DEPs shows a larger size (Fig. 3F). The PI of DEPs in the ATP vs. IP comparison is higher (Fig. 3G). Additionally, the median GARVY for upregulated DEPs in the ATP vs. IP comparison is notably lower, at −0.27 (Fig. 3H and Table S6).

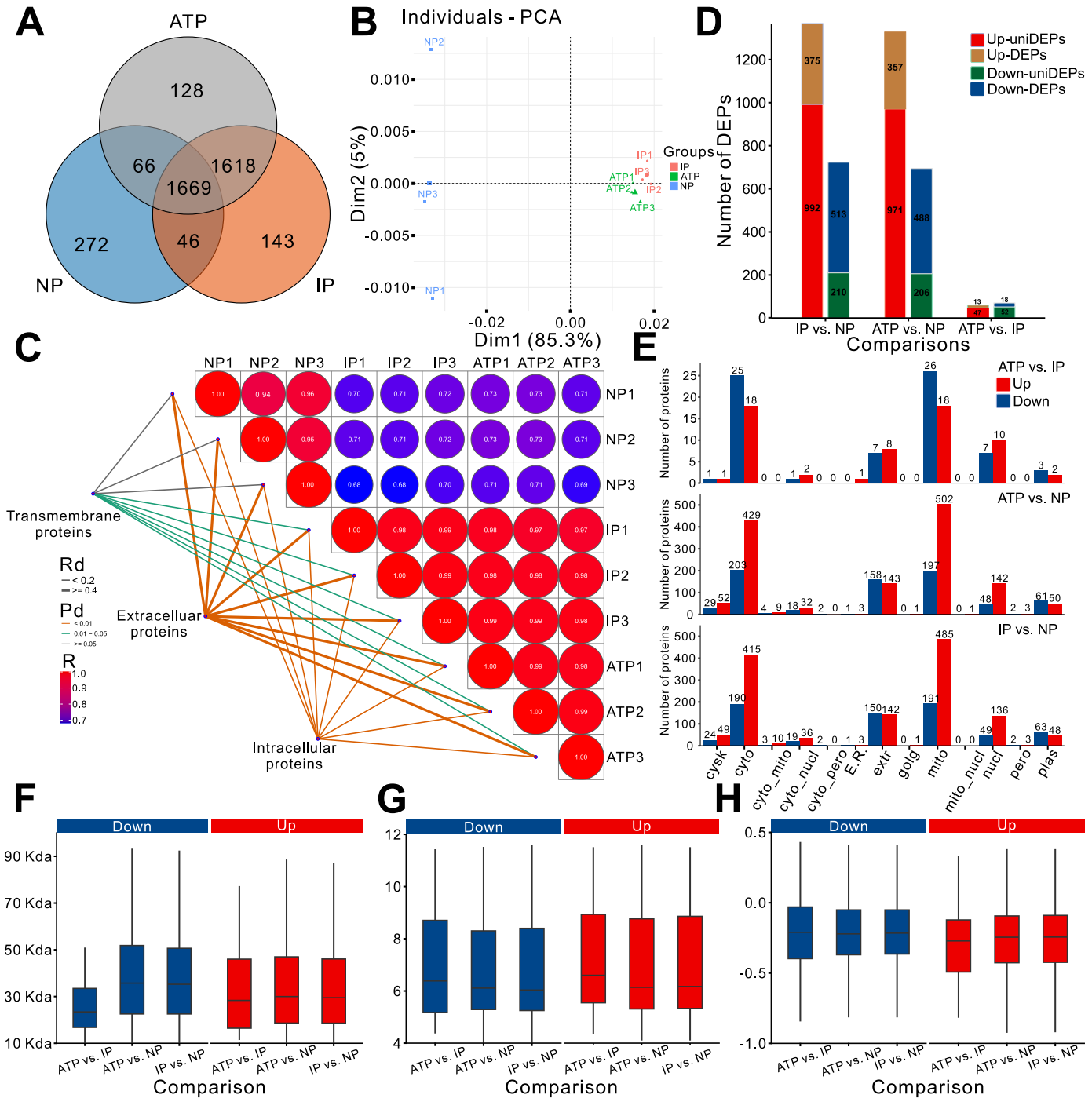

Fig. 3. Analysis of the proteome data from *A. pacificum* under different P conditions. (A) Venn diagram of the number of shared and unique proteins among the treatments. Analyze correlation using the method of PCA (B) and PCC (C) with cellular localization. (D) The distribution of upregulated and downregulated DEPs across comparisons was analyzed. Subcellular localization (E), molecular weight (F), isoelectric point (G), and GRAVY (H) of up and downregulated DEPs among comparisons were identified.

3.4. Proteomic responses of *A. pacificum* to various P

We conducted a GO and KEGG enrichment analysis on *A. pacificum* proteins bound to various P compounds, to elucidate the functional roles of the DEPs. The main GO categories included catalytic activity, binding, and oxidoreductase activity under Molecular Functions; plastid, membrane, and thylakoid within Cellular Components; metabolic processes, responses to stimuli, and catabolic processes under Biological Processes (Figs. S3C and S4A and Tables S7–9). We analyzed the top 10 upregulated and downregulated pathways in comparison. P-replete groups exhibited enrichment of upregulated DEPs in the ribosome (ko03010), glycine, serine and threonine metabolism (ko00260), and other pathways, while downregulated DEPs in pathways involving protein secretion (ko03060), glycolysis/gluconeogenesis (ko00010) and peroxisome (ko04146) (Figs. S3D and S4B and Table S15).

Therefore, under various P treatments, *A. pacificum* exhibited differential expression of proteins associated with many pathway such as transmembrane transport, cellular growth, and toxin biosynthesis. Notably, ACP showed a 10.59-fold upregulation under P-deficient condition, indicative of enhanced phosphoester hydrolysis capacity (Fig. 4,

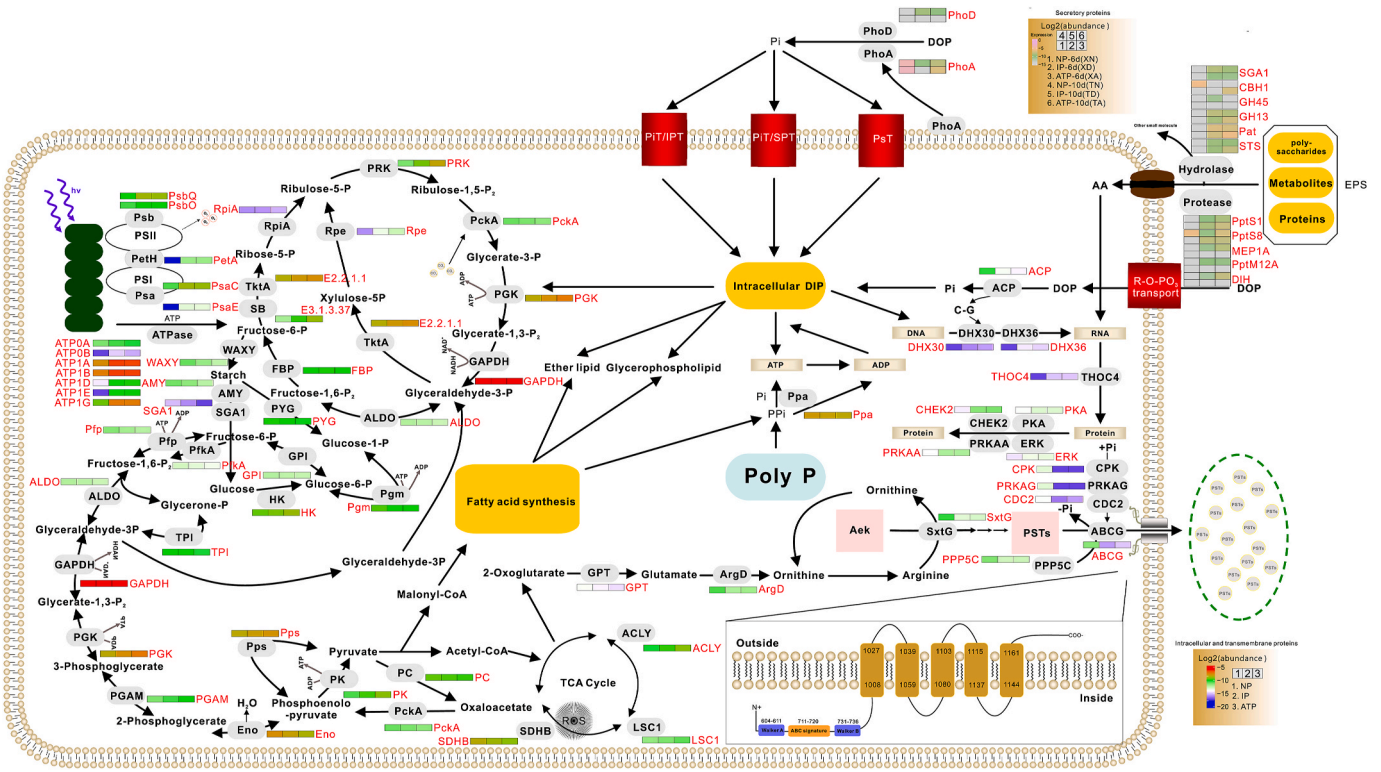

Fig. 4. Molecular mechanisms response to P uptake and metabolism in *A. pacificum* under various P conditions. Their expression changes in all comparisons are displayed with the color indicator for the $\log_2$(fold change) at the right (In the upper right lies the protein group for secretome, while in the lower right lies the proteome). The protein expression amount was the sum of the abundance of all relevant DEPs, and function annotation of DEPs see suptable S16. (For interpretation of the references to color in this figure legend, the reader is referred to the Web version of this article.)

Table S16). ACP is an induced enzyme, that participates in both intracellular and extracellular non-specific hydrolase of organic phosphates, facilitating the synthesis and circulation of inorganic P. The activity formed intracellularly might relate to the phosphate source within paramylum granules (Sommer and Blum, 1965; Zhang et al., 2019a).

Splicing factors DHX30 and DHX36 are significantly reduced under P-deficient condition (Fig. 4, Table S16), and the spliceosome is responsible for removing introns from pre-mRNA transcribed from the genome in eukaryotic cells (Will and Luhrmann, 2011). Furthermore, THOC4 is similarly reduced, a subunit of the THO complex that is involved in the exon-joining process of pre-mRNA (Hir et al., 2016). P-deficiency inhibits the expression process of the alkaline phosphatase gene, and at the same time, protein kinases like mitogen-activated protein kinase (ERK) and protein kinase A (PKA) were also suppressed (Fig. 4). These proteins interact with downstream proteins through phosphorylation activation, thereby controlling signal transduction between metabolic pathways (Sopory and Munshi, 1998). The protein kinase activity of *Alexandrium catenella* would change under P-deficient condition (Zhang et al., 2014), and post-translational protein phosphorylation regulates the circadian rhythm of protein expression in dinoflagellates (Roy et al., 2014; Akbar et al., 2023).

Photosynthetic microalgae due to their efficient photosynthesis, emerge as potential contributors to biomass (De Bhowmick et al., 2019). In our study, the downregulated proteins involved in photosynthesis included PsaC, PsaE from photosystem I, PsbO, PsbQ from photosystem II, and apocytochrome protein PetA (Fig. 4, Table S16). Consequently, the capacity of *A. pacificum* to acquire and transmit electrons is diminished in P-deficient group. In particular, proteins (ATPF0A, ATPF0B, ATPF1A, ATPF1B, ATPF1D, ATPF1E, ATPF1G) related to ATPase were downregulated in P-deficient group (Fig. 4), exacerbating a decline in cellular energy production efficiency. This is likely because P-deficiency restricts photophosphorylation, resulting in reduced ATP output and, consequently, inefficient operation of photosynthesis (Chen et al., 2024).

The synthesis of PSTs in related dinoflagellates is influenced by factors such as temperature, light, salinity, and nutrient availability (Bui et al., 2024). Among these, a lack of P can lead to an increase in the cellular quotas of PSTs (Zhang et al., 2019a), and arginine is a crucial precursor for the synthesis of PSTs (Anderson et al., 1990). The expression of alanine transaminase (GPT) and acetylornithine aminotransferase (ArgD) enhances the conversion efficiency of arginine in P-deficient group. Moreover, the suppression of cell proliferation due to P-deficiency generates more readily available arginine (Zhang et al., 2019a). Amidinotransferase encoded by *SxtG* gene is one of the core proteins in the synthesis of PSTs which significantly upregulated in P-deficient group (Fig. 4, Table S16), catalyzing the binding of arginine and imidazole group from the product of *SxtA* gene, and releasing ornithine (Bui et al., 2024; Kim et al., 2024). In response to cold stress, the accumulation of PSTs is associated with a significant rise in the expression of *SxtG* gene in *A. pacificum* (Wang et al., 2022), indicates that SxtG plays a pivotal role in boosting the synthesis of PSTs under conditions of P-deficiency. Overall, these findings suggest that SxtG is possibly primarily regulated by the arginine synthesis process involving the TCA cycle product, 2-oxoglutarate (Chen et al., 2024).

The ABC (ATP-binding cassette) transporter family proteins facilitate substrate transmembrane transport by harnessing the energy released from ATP hydrolysis, exhibiting broad substrate selectivity (Davidson et al., 2008). The *Microcystis aeruginosa* enables the secretion and extrusion of toxic secondary metabolites or derivatives out of the cell through ABC transporters (Pearson et al., 2004). Similarly, plants can utilize ABCG proteins for the expulsion of toxic substances and external pollutants (Kretzschmar et al., 2011). We detected a semi-structured ABCG protein (TRINITY_DN109_c0_g1_i2.p1) with significantly elevated expression in P-deficient group (Fig. 4). ABC transporters have

been established to serve as carriers for okadaic acid (OA) (Svensson et al., 2003). In the study of *Prorocentrum lima*, an upregulation of ABCG protein under nitrogen limitation conditions was observed and possibly relevant to OA transportation (Hou et al., 2018). Coupled with the increased content of *A. pacificum* PSTs in cells under P-deficient condition suggest that ABCG may play a role in the transmembrane transport of PSTs (Chen et al., 2024).

3.5. WGCNA analysis for DEPs of proteome

WGCNA clustered proteins into 11 different modules, each distinguished and visually represented by a distinct color. DEPs distributions are illustrated through heatmaps (Fig. 5A, Table S17), and correlations between modules and groups were calculated. The MEblue module ($P = 0.0048$, Trait correction 0.837) was highly associated with ATP - NP group, while the MEblack, magenta, pink, red, and green modules showed significant correlations exceeding 0.77 with ATP - IP group. Interactions were noted among the MEred, magenta, and green modules (Fig. S5A). There are 775 and 31 DEPs within the MEblue and red modules, respectively. Identifying hub DEPs within these modules indicates their crucial roles, given their important network positions and high connectivity (Table S17).

The STRING database was used to annotate the functions of the proteins in the MEblue and MEred modules. Within the MEred module, the core DEP identified is glycine lyase (GcvP, TRINITY_DN18192_c0_g3_i1.p1), interconnected with two DEPs respectively are diphosphate reductase (IspH, TRINITY_DN44687_c0_g1_i1.p1) and succinate-CoA ligase (SUCL, TRINITY_DN112950_c0_g1_i1.p1). DEPs related to photosynthesis connected to the MEblue network, including PsaA (TRINITY_DN4015_c0_g1_i1.p1), PsaF (TRINITY_DN364_c0_g1_i14.p1), PsbU (TRINITY_DN3216_c0_g1_i35.p1), and PsbV (TRINITY_DN430_c0_g1_i16.p1), associated with core DEPs NAD (P)-linked oxidoreductase (TRINITY_DN16039_c0_g2_i1.p1) (Fig. 5B).

PhoA has been grouped into the MEblue module. It was found that PhoA interacts with 5′-nucleotidase (TRINITY_DN8685_c0_g1_i1.p1) and various oxidoreductase-related proteins (TRINITY_DN177157_c0_g1_i1.p1, TRINITY_DN149643_c0_g1_i1.p1, TRINITY_DN207327_c0_g1_i1.p1 and TRINITY_DN213641_c0_g1_i1.p1) (Fig. S5B). There could be a cooperative interaction among them, jointly participating in the process of organic P metabolism. Protein interaction analysis reveals a stronger correlation between SxtG and DEPs related to the TCA cycle, including AcnB (TRINITY_DN1027_c0_g2_i6.p1), CS (TRINITY_DN2340_c0_g1_i4.

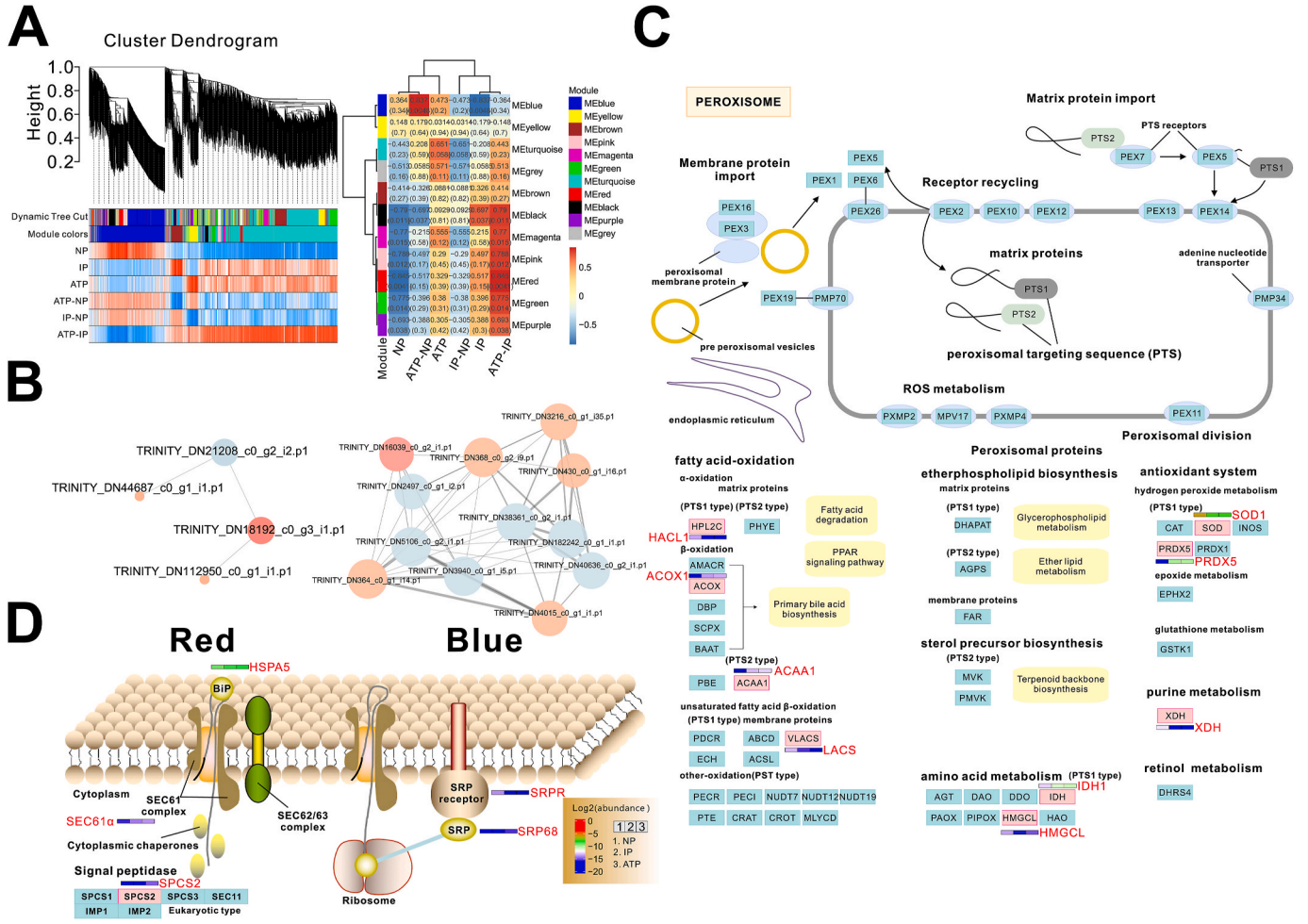

Fig. 5. WGCNA clustered functionally highly correlated proteins into the same module and the modules highly related to the treatment were screened out. (A) The protein module and trait-associated diagram showed that the proteins are divided into 11 modules and designated with specific colors, and the heatmap showed the spread of the DEPs in different treatments. The upper number is the Person correlation value and the number below is the P-value of the module and treatment. (B) The co-expression network diagrams of the proteins from the MEred and MEblue, Node size stands for the connectivity value of proteins, and the width of a straight line stands for the weight value. Red nodes represent hubDEPs, orange nodes represent DEPs, and blue nodes represent nondifferential proteins. (C) The expression analysis of DEPs related to peroxisomes and the enzymes associated with DEPs are marked with pink boxes, (D) and DEPs associated with protein excretion pathways are highlighted in red characters. The color indicators for $\log_2$(fold change) for comparisons are shown in the middle bottom. (For interpretation of the references to color in this figure legend, the reader is referred to the Web version of this article.)

p1), and SDHA (TRINITY_DN601_c0_g1_i1.p1) (Fig. S5B). Furthermore, ABCG proteins were detected in the MEblue module and demonstrated a high correlation with protein kinases (CPK (TRINITY_DN18699_c0_g2_i1.p1), CDC2 (TRINITY_DN9464_c0_g2_i2.p1), and PRKAG (TRINITY_DN43799_c0_g1_i2.p1)) (Fig. S5B). It's worth noting that all three proteins exhibit an expression pattern similar to that of ABCG in P-deficient group (Table S4), suggesting a plausible direct involvement in the regulation of phosphorylation for the ABCG protein.

4. Discussion

Over the past few decades, global concerns have risen due to the increased occurrence of harmful algae, which pose threats to both aquatic ecosystems and human health (Abassi et al., 2023). Moreover, the capacity to assimilate organic P is recognized as a key driver in the initiation of harmful algal blooms (Jauzein et al., 2010; Wang et al., 2011; He et al., 2016). ATP serves as a crucial component among DOP forms within marine ecosystems, frequently encountered at elevated levels in aquatic environments (Nawrocki and Karl, 1989). In this study, we investigated the protein profiles of *A. pacificum* that respond to various P compounds. Notably, P-replete groups exhibited a higher abundance of unique proteins in both proteome and secretome, indicating that different P compounds affect the expression of specific proteins (Figs. 2 and 3). Growth rate and photosynthetic performance significantly decrease under P-deficiency, culminating in a cell density capped at $0.36 \pm 0.01 \times 10^3$ cells mL^{-1}, and cell diameter augmentation nearly double to P-replete groups (Vaulot et al., 1996). Photosynthesis and growth parameters remained largely unchanged across P-replete groups, implying that *A. pacificum* can effectively utilize ATP under P-deficiency (Chen et al., 2024). This insight offers a rationale for the occurrence of toxic algal blooms in ecosystems heavily impacted by human activity.

4.1. Various P affects the peroxisome

Peroxisomes (ko04146) exhibit a range of metabolic functions such as fatty acid degradation, detoxification of reactive oxygen species (ROS), and synthesis of ether phospholipids. These compartments integrate parts of biochemical pathways, but usually, peroxisomes coexist with other cellular components to form intricate networks (Fransen et al., 2017; Mix et al., 2018). In this study, 30 DEPs in this pathway were analyzed, which is mainly related to isocitrate dehydrogenase (IDH1, 7 proteins), superoxide dismutase Cu-Zn family (SOD1, 12 proteins), and acyl-CoA oxidase (ACOX1, 3 proteins) (Fig. 5C). NADPH is indispensable for maintaining cellular redox equilibrium. IDH1 facilitates the oxidation-decarboxylation of isocitrate, yielding NADPH, which is reduced in P-deficient group. Consequently, the diminished number of cofactors essential for reactive nitrogen species (RNS) and ROS metabolism leads to peroxisome modification, which might compromise the cell's defense against oxidative stress (Sandalio and Romero-Puertas, 2015; Leterrier et al., 2016). ACOX1 is a crucial protein in fatty acid β-oxidation, facilitating the conversion of acyl-CoA into acetyl-CoA through esterification (Wu et al., 2023). Its undetectable presence during P-deficient group could result in a diminished yield of acetyl-CoA, with potential consequences for the TCA cycle and other metabolic pathways (Fig. 5C). Long-chain acyl-CoA synthetase (LACS1) was upregulated in ATP group, which facilitates the conversion of free fatty acids into acyl-CoA via ATP-coupling, a critical step in lipid metabolism encompassing fatty acid transport, synthesis, and β-oxidation (Wu et al., 2020). Decreasing the expression of LACS1 reduces triacylglycerol (TAG) synthesis, implying that TAG could potentially accumulate intracellularly in the form of lipid droplets (Bai et al., 2022; Li et al., 2024).

4.2. Various P affects the protein export

Many hydrophilic and soluble proteins, membrane proteins, and secreted proteins require passage through or incorporation into the membranes of the eukaryotic endoplasmic reticulum (Nelson and Yeaman, 2001; Mitra et al., 2004). These proteins utilize the translocon within the endoplasmic reticulum known as PCC, which facilitates crossing the phospholipid bilayer by overcoming the energy barrier. Sec61αβγ forms a heterotrimeric core, there is a pronounced elevation of Sec61α expression in ATP group. The absence or degradation of Sec61α results in significant suppression of the signal recognition particle (SRP)-mediated pathway (Raden et al., 2000). There are 11 DEPs enriched in soluble chaperone BiP, which facilitates precursor protein transport through translocases (Mitra et al., 2006). P-deficient group is marked by notably diminished BiP levels, indicating that the post-translational translocation of the *A. pacificum* is inhibited under P-deficiency (Fig. 5D). Proteins with more hydrophobic signal peptides have a higher propensity to associate with SRP. This binding facilitates the interaction between the RNC and the α-subunit of the SRP receptor (SRPR) located on the endoplasmic reticulum during the cotranslational translation process, promoting their subsequent processing and modification (Eisner et al., 2003; Mitra et al., 2006). The upregulation of SRPR in P-deficient group suggests an enhancement of the co-translational translocation pathway. In the meantime, a higher median hydrophobicity values of the signal peptide were found in secretory proteins (Fig. S5C), which may imply that secretory proteins to be mainly processed by SRP components in *A. pacificum*. The expression of SPC2 in the ATP group may contribute to protein processing within the ER (Fig. 5D), as a non-essential subunit of the signal peptidase complex, where it contributes to and supports the redundancy in signal peptide cleavage and membrane protein degradation processes (Mullins et al., 1996). SRP68 was upregulated under ATP group, owing to its central role as a component of the SRP (Grotwinkel et al., 2014), it might improve the efficiency of the co-translational translation pathway in processing secretory proteins and membrane proteins, but the specific functional proteins involved in this process require further investigation.

4.3. Energy metabolism

Photosynthetic products are mainly stored as starch in cells to reduce P consumption under P-deficient condition (Poirier and Bucher, 2002). Glycogen phosphorylase (PYG) catalyzes the direct conversion of starch into α-D-glucose-1P, alongside alpha-amylase (AMY) and glucoamylase (SGA1) upregulation in P-deficient group, enhances the efficiency of starch conversion into D-glucose. The upregulated expression of glyceraldehyde-3-phosphate dehydrogenase (GAPDH) suggests that more NADH was produced by catalyzing the conversion of 3-phosphoglyceraldehyde to glyceraldehyde-1,3-bisphosphate (Ghuffar et al., 2018; Huang et al., 2018). However, the downregulation of pyruvate kinase (PK) and phosphoglycerate kinase (PGK) which as key proteins in glycolysis (Fig. 4, Table S16), indicates that the energy-producing processes are still being inhibited (Zhang et al., 2019a). Phosphoribulokinase (PRK) participates in the final step of the Calvin cycle, through irreversible catalysis of ribulose-5-phosphate into ribulose-1, 5-bisphosphate, ensures the continuous operation of the cycle (Rumpho et al., 2009). In P-deficient group, phosphoglycerate kinase (PGK), phosphoribulokinase (PRK), and ribose 5-phosphate isomerase A (RpiA) in the Calvin cycle were downregulated (Fig. 4), which led to a decrease in carbon fixation and consumption of cellular ATP (Sharwood et al., 2016; Zhang et al., 2019a). The fructose-bisphosphate aldolase (ALDO) were upregulated when P was limited, and proteins related to the upstream of 1,6-bisphosphate fructose in glycolysis also upregulated, including diphosphate-dependent phosphofructokinase (Pfp), 6-phosphofructokinase A (PfkA) and phosphoglucomutase (Pgm), indicating when the Calvin cycle's functionality is compromised or inefficient by P-deficiency, alternative routes are potentially available for the

replenishment of its intermediate metabolite. With glycolytic shunts, Utilizing cellular carbohydrate reservoirs to supplement the cycle (Gutekunst, 2018; Makowka et al., 2020).

TCA cycle-related protein, succinyl-CoA synthetase (LSC1) and ATP citrate (pro-S)-lyase (ACLY) were non-comparable across the ATP and IP groups (Fig. 4), suggesting *A. pacificum* did not escalate its energy synthesis to fulfill metabolic requirements when treated with ATP (Chen et al., 2024). The succinate dehydrogenase (ubiquinone) iron-sulfur subunit (SDHB) belongs to mitochondrial inner membrane proteins, serving as a critical component of the succinate dehydrogenase (SDH) catalytic domain (Moosavi et al., 2019). Due to its role in the TCA cycle and involvement in ROS production through the electron transport chain (Jardim-Messeder et al., 2015), the higher expression in the ATP group might potentially enhance the immunomodulatory function of *A. pacificum*. Specifically, the upregulation of pyruvate carboxylase (PC) and phosphoenolpyruvate carboxykinase (PckA) in P-deficient group, indicates that P-deficient group might enhance the interaction between glycolysis and the TCA cycle through a conversion between oxaloacetate, pyruvic acid, and phosphoenolpyruvate. In conclusion, ATP enhances the yield of FADH2 in the TCA cycle compared to the IP group (Yang et al., 2020), and *A. pacificum* cells initiated the regulation of phosphate consumption to achieve equilibrium with its energetic demands like glycolysis (Wurch et al., 2011), underscoring the adaptive pressure exerted by P fluctuation on the *A. pacificum*.

4.4. Secretory protein

Alkaline phosphatase (AP) acts as a broad-spectrum phosphomonoesterase that facilitates the hydrolysis of diverse phosphate esters (Ren et al., 2017), functioning as a crucial enzyme for phytoplankton to harness DOP when the supply of DIP is restricted (Lin et al., 2012a). In the present study, we observed a significant elevation in both cytoplasmic and extracellular APA levels in P-deficient group, associated with a notable increase in the expression of PhoA in proteome and secretome (Chen et al., 2024). PhoD exhibits significantly higher expression in P-replete groups, as time progresses, this corresponds to the trend of extracellular APA in the ATP group (Figs. 1E and 4). In particular, we have found that PhoA contains a transmembrane domain (32–51) that is close to the signal peptide sequence (1–25). In certain instances, signal peptides may remain uncleaved and facilitate the protein's anchoring within the phospholipid bilayer (Cho et al., 2009). This proximity of location might explain why there is a higher abundance detectable intracellularly. There is a certain level of weak attachment to the cell wall, its main function appears to be extracellular (Fig. 4). Additional analyses of the secretome uncovered detached wall proteins resulting from their weak association with the cell wall (Cho et al., 2009; Choi et al., 2021).

This study investigates that various extracellular proteases capable were detected in P-replete groups (Wang et al., 2020). Besides, serine protease is uniquely expressed in the TD and TA cultures (Fig. 4), it has been documented that they can activate the activity of secreted proteins by cleaving them, thus enhancing the function of these secreted proteins in yeast (Ladds and Davey, 2000). Furthermore, it has been found that Pat, Dlh, and several glycosidases are notably absent in P-deficient group (Fig. 4, Table S16). Some studies indicate that Pat modulates plant tissue defense responses by regulating cell wall porosity and altering levels of defense-related hormones and metabolites, with its expression significantly upregulated under salt stress (Shahin et al., 2023). The DlH family suppresses biofilm replication, DlH3 (a protein screened from microalgae) exhibits 54.5 % inhibitory activity against *Edwardsiella anguillarum*. Furthermore, DlH3 upregulates defense-associated functions, including genes encoding efflux mechanisms and transport system activities (Bergmann et al., 2024). These findings collectively demonstrate that P-deficiency compromises cellular defense and stress resilience in *A. pacificum*, but conversely enhances organic P utilization capacity, consistent with prior studies (Luo et al., 2017; Chen et al., 2024).

5. Conclusions

The current study explores the molecular response mechanisms of *A. pacificum* under various P conditions by comparative proteome and secretome analysis. These findings indicate that P-deficiency has negative effects on the growth and photosynthesis of *A. pacificum*. PhoA is upregulated significantly in both P-deficient and ATP groups, and PhoD is specifically expressed in P-replete groups. Acid phosphatase (ACP) could be the principal mechanism for the utilization of intracellular organic P, suggesting that *A. pacificum* exhibits a strong capacity to utilize DOP. Furthermore, *A. pacificum* may compensate for the consumption of Calvin cycle intermediates via alternative carbon metabolism processes, especially when the process of photosynthetic carbon fixation was inhibited by P-deficiency. In summary, *A. pacificum* not only enhances its ability to acquire various forms of DOP but also adapts to low-P environments through different strategies including efficiently regulating cellular metabolism and P distribution. Our data demonstrate that *A. pacificum* thrives under these conditions by (1) maintaining growth via ATP hydrolysis even when DIP is scarce, (2) compensating for Calvin cycle intermediate depletion through alternative carbon metabolism under P-deficiency-induced photosynthetic inhibition, (3) minimizing extracellular carbon loss through reduced EPS metabolism, and (4) enhancing PSTs synthesis as a potential allelopathic strategy. These adaptive mechanisms likely contribute to the increasing frequency and persistence of *A. pacificum* blooms in nutrient-imbalanced coastal systems, where DOP serves as both a phosphorus reservoir and a selective advantage over less versatile phytoplankton.

CRediT authorship contribution statement

Xiaohang Li: Writing – original draft, Software, Methodology, Formal analysis. **Xi Chen:** Writing – original draft, Visualization, Supervision, Resources. **Shuxue Zhao:** Methodology, Data curation. **Hua Jiang:** Methodology. **Yuqin Cai:** Methodology. **Jie Bai:** Conceptualization. **Jiajun Shao:** Methodology. **Hao Yu:** Supervision, Software, Formal analysis. **Tiantian Chen:** Writing – review & editing, Funding acquisition, Conceptualization.

Declaration of competing interest

The authors declare that they have no known competing financial interests or personal relationships that could have appeared to influence the work reported in this paper.

Acknowledgments

This study was supported by the Fundamental Research Funds for the Central Universities (202413029), and Qingdao Agricultural University Scientific Research Foundation (6602423332). We wish to thank Key Laboratory of Marine Environment and Ecology, Ocean University of China and Central Laboratory of School of Life Science, Qingdao Agricultural University.

Abbreviation:

α	initial slope of the photosynthesis efficiency
ABCG	ABC transporter G family protein
ACP	acid phosphatase
APA	alkaline phosphatase activity
DEPs	differentially expressed proteins
DIP	dissolved inorganic P
DOP	dissolved organic P
EPS	extracellular polymeric substances
ESD	equivalent spherical diameter

HABs	harmful algal blooms
I_k	half-saturation light intensity
IP	NaH_2PO_4 treatment
NP	P-deficient treatment
OA	okadaic acid
P	Phosphorus
PhoA	alkaline phosphatase A
PhoD	alkaline phosphatase D
PST	phosphate starvation transcript
PSTs	paralytic shellfish toxins
rETRmax	maximum photosynthesis rate at maximum electron transfer efficiency
RLC	light-response curve
RNC	ribosome-nascent polypeptide complex
SRP	signal recognition particle
SRPR	SRP recepter
SxtG	Amidinotransferase
TA	ATP treatment on day 10
TD	NaH_2PO_4 treatment on day 10
TDP	total dissolved P
TN	P-deficient treatment on day 10
WGCNA	Weighted Gene Co-Expression Network Analysis
XA	ATP treatment on day 6
XD	NaH_2PO_4 treatment on day 6
XN	P-deficient treatment on day 6

Appendix A. Supplementary data

Supplementary data to this article can be found online at https://doi.org/10.1016/j.envpol.2025.126135.

Data availability

I have shared the link to my data at the data availability in manuscript

References

Abassi, S., Kim, H.S., Bui, Q.T.N., Ki, J.S., 2023. Effects of nitrate on the saxitoxins biosynthesis revealed by *sxt* genes in the toxic dinoflagellate *Alexandrium pacificum* (group IV). Harmful Algae 127, 102473. https://doi.org/10.1016/j.hal.2023.102473.

Akbar, M.A., Mohd Yusof, N.Y., Usup, G., Ahmad, A., Baharum, S.N., Bunawan, H., 2023. Nutrient deficiencies impact on the cellular and metabolic responses of saxitoxin producing *Alexandrium minutum*: a Transcriptomic Perspective. Mar. Drugs 21, 497. https://doi.org/10.3390/md21090497.

Anderson, D.M., Kulis, D.M., Sullivan, J.J., Hall, S., Lee, C., 1990. Dynamics and physiology of saxitoxin production by the dinoflagellates *Alexandrium* spp. Mar. Biol. 104, 511–524. https://doi.org/10.1007/BF01314358.

Bai, F., Yu, L., Shi, J., Li-Beisson, Y., Liu, J., 2022. Long-chain acyl-CoA synthetases activate fatty acids for lipid synthesis, remodeling and energy production in Chlamydomonas. New Phytol. 233, 823–837. https://doi.org/10.1111/nph.17813.

Bergmann, L., Balzer Le, S., Hageskal, G., Preuss, L., Han, Y., Astafyeva, Y., Loevenich, S., Emmann, S., Perez-Garcia, P., Indenbirken, D., Katzowitsch, E., Thümmler, F., Alawi, M., Wentzel, A., Streit, W.R., Krohn, I., 2024. New dienelactone hydrolase from microalgae bacterial community-Antibiofilm activity against fish pathogens and potential applications for aquaculture. Sci. Rep. 14, 377. https://doi.org/10.1038/s41598-023-50734-9.

Bui, Q.T.N., Pradhan, B., Kim, H.S., Ki, J.S., 2024. Environmental factors modulate saxitoxins (STXs) production in toxic dinoflagellate *Alexandrium*: an updated review of STXs and synthesis gene aspects. Toxins 16, 210. https://doi.org/10.3390/toxins16050210.

Casey, J.R., Lomas, M.W., Michelou, V.K., Dyhrman, S.T., Orchard, E.D., Ammerman, J. W., Sylvan, J.B., 2009. Phytoplankton taxon-specific orthophosphate (Pi) and ATP utilization in the western subtropical North Atlantic. Aquat. Microb. Ecol. 58, 31–44. https://doi.org/10.3354/ame01348.

Chen, T., Chen, X., Sun, H., Zhang, H., Bai, J., 2024. Unveiling the responses of *Alexandrium pacificum* to phosphorus utilization by physiological and transcriptomic analysis. Sci. Total Environ. 911, 168759. https://doi.org/10.1016/j.scitotenv.2023.168759.

Cho, W.K., Chen, X.Y., Chu, H., Rim, Y., Kim, S., Kim, S.T., Kim, S.W., Park, Z.Y., Kim, J. Y., 2009. Proteomic analysis of the secretome of rice calli. Physiol. Plantarum 135, 331–341. https://doi.org/10.1111/j.1399-3054.2008.01198.x.

Choi, J., Shin, J.H., An, H.J., Oh, M.J., Kim, S.R., 2021. Analysis of secretome and N-glycosylation of *Chlorella* species. Algal Res. 59, 102466. https://doi.org/10.1016/j.algal.2021.102466.

Davidson, A.L., Dassa, E., Orelle, C., Chen, J., 2008. Structure, function, and evolution of bacterial ATP-binding cassette systems. Microbiol. Mol. Biol. Rev. 72, 317–364. https://doi.org/10.1128/MMBR.00031-07.

De Bhowmick, G., Sarmah, A.K., Sen, R., 2019. Zero-waste algal biorefinery for bioenergy and biochar: a green leap towards achieving energy and environmental sustainability. Sci. Total Environ. 650, 2467–2482. https://doi.org/10.1016/j.scitotenv.2018.10.002.

Dyhrman, S., Ammerman, J., Van Mooy, B., 2007. Microbes and the marine phosphorus cycle. Oceanography (Wash., D.C.) 20, 110–116. https://doi.org/10.5670/oceanog.2007.54.

Dyhrman, S.T., 2016. Nutrients and their acquisition: phosphorus physiology in microalgae. In: Borowitzka, M.A., Beardall, J., Raven, J.A. (Eds.), The Physiology of Microalgae. Springer International Publishing, Cham, pp. 155–183. https://doi.org/10.1007/978-3-319-24945-2_8.

Eisner, G., Koch, H.-G., Beck, K., Brunner, J., Müller, M., 2003. Ligand crowding at a nascent signal sequence. J. Cell Biol. 163, 35–44. https://doi.org/10.1083/jcb.200306069.

Fransen, M., Lismont, C., Walton, P., 2017. The peroxisome-mitochondria connection: how and why? Int. J. Mol. Sci. 18, 1126. https://doi.org/10.3390/ijms18061126.

Ge, J., Yang, Q., Fang, Z., Liu, S., Zhu, Y., Yao, J., Ma, Z., Gonçalves, R.J., Guan, W., 2022. Microplastics impacts in seven flagellate microalgae: role of size and cell wall. Environ. Res. 206, 112598. https://doi.org/10.1016/j.envres.2021.112598.

Ghuffar, S., Irshad, G., Naz, F., Rosli, H.B., Hyder, S., Mehmood, N., Zeshan, M.A., Raza, M.M., Mayer, C.G., Gleason, M.L., 2018. First report of two *Penicillium* spp. causing postharvest fruit rot of grapes in Pakistan. Plant Dis. 102. https://doi.org/10.1094/PDIS-10-17-1616-PDN, 1037-1037.

Guillard, R.R.L., Ryther, J.H., 1962. Studies of marine planktonic diatoms: I. Cyclotella nana Hustedt, and Detonula confervacea (Cleve) gran. Can. J. Microbiol. 8, 229–239. https://doi.org/10.1139/m62-029.

Gong, W., Browne, J., Hall, N., Schruth, D., Paerl, H., Marchetti, A., 2017. Molecular insights into a dinoflagellate bloom. ISME J. 11, 439–452. https://doi.org/10.1038/ismej.2016.129.

Grotwinkel, J.T., Wild, K., Segnitz, B., Sinning, I., 2014. SRP RNA remodeling by SRP68 explains its role in protein translocation. Science 344, 101–104. https://doi.org/10.1126/science.1249094.

Gutekunst, K., 2018. Hypothesis on the synchronistic evolution of autotrophy and heterotrophy. Trends Biochem. Sci. 43, 402–411. https://doi.org/10.1016/j.tibs.2018.03.008.

Hallegraeff, G.M., 2003. Harmful algal blooms: a global overview. Manual on harmful marine microalgae 33, 1–22.

He, D., Chao, J., Zhang, Y., Yang, F., Wang, Y., Guo, Y., 2016. Effects of the phytoplankton-derived particulate organic matter on the growth and phosphorus enrichment of phosphorus-deficiency *Microcystis aeruginosa*. China Environ. Sci. 36, 3777–3783. https://doi.org/10.0000/j.zghjkx.1000-6923.20163614916.

Hir, H.L., Saulière, J., Wang, Z., 2016. The exon junction complex as a node of post-transcriptional networks. Nat. Rev. Mol. Cell Biol. 17, 41–54. https://doi.org/10.1038/nrm.2015.7.

Hou, D., Mao, X., Gu, S., Li, H., Liu, J., Yang, W., 2018. Systems-level analysis of metabolic mechanism following nitrogen limitation in benthic dinoflagellate *Prorocentrum lima*. Algal Res. 33, 389–398. https://doi.org/10.1016/j.algal.2018.06.004.

Houliez, E., Lefebvre, S., Lizon, F., Schmitt, F.G., 2017. Rapid light curves (RLC) or non-sequential steady-state light curves (N-SSLC): which fluorescence-based light response curve methodology robustly characterizes phytoplankton photosynthetic activity and acclimation status? Mar. Biol. 164, 175. https://doi.org/10.1007/s00227-017-3208-8.

Huang, B., Ou, L., Wang, X., Huo, W., Li, R., Hong, H., Zhu, M., 2007. Alkaline phosphatase activity of phytoplankton in East China Sea coastal waters with frequent harmful algal bloom occurrences. Aquat. Microb. Ecol. 49, 195–206. https://doi.org/10.3354/ame01135.

Huang, D., Cheng, C.Q., Qiu, J.B., Huang, Y., Zhang, H.Y., Xu, Z.H., Wu, S.W., Huang, Y. T., Chen, J., Zou, L.G., Yang, W.D., Zheng, X.F., Li, H.Y., Li, D.W., 2024. Mechanistic insights into the effects of diuron exposure on *Alexandrium pacificum*. Water Res. 250, 120987. https://doi.org/10.1016/j.watres.2023.120987.

Huang, L., Zhu, Y.N., Yang, J.Y., Li, D.W., Li, Y., Bian, L.M., Ye, J.R., 2018. Shoot blight on Chinese fir (*Cunninghamia lanceolata*) is caused by *Bipolaris oryzae*. Plant Dis. 102, 500–506. https://doi.org/10.1094/PDIS-07-17-1032-RE.

Jardim-Messeder, D., Caverzan, A., Rauber, R., De Souza Ferreira, E., Margis-Pinheiro, M., Galina, A., 2015. Succinate dehydrogenase (mitochondrial complex II) is a source of reactive oxygen species in plants and regulates development and stress responses. New Phytol. 208, 776–789. https://doi.org/10.1111/nph.13515.

Jauzein, C., Labry, C., Youenou, A., Quéré, J., Delmas, D., Collos, Y., 2010. Growth and Phosphorus uptake by the toxic dinoflagellate *Alexandrium catenella* (dinophyceae) in response to phosphate limitation 1. J. Phycol. 46, 926–936. https://doi.org/10.1111/j.1529-8817.2010.00878.x.

Jeffries, D., Dieken, F., Jones, D., 1979. Performance of the autoclave digestion method for total phosphorus analysis. Water Res. 13, 275–279. https://doi.org/10.1016/0043-1354(79)90206-9.

Jin, W.Y., Chen, X.W., Tan, J.Z., Lin, X., Ou, L.J., 2023. Variation in intracellular polyphosphate and associated gene expression in response to different phosphorus conditions in the dinoflagellate *Karenia mikimotoi*. Harmful Algae 129, 102532. https://doi.org/10.1016/j.hal.2023.102532.

Karl, D.M., 2000. Phosphorus, the staff of life. Nature 406, 31–33. https://doi.org/10.1038/35017683.
Kim, H.S., Bui, Q.T.N., Shin, J., Wang, H., Ki, J.S., 2024. Promoter regions of *sxtA* and *sxtG* reveal relationship between saxitoxin biosynthesis and photosynthesis in toxic *Alexandrium catenella*. J. Appl. Phycol. 36, 1181–1195. https://doi.org/10.1007/s10811-023-03159-w.
Kretzschmar, T., Burla, B., Lee, Y., Martinoia, E., Nagy, R., 2011. Functions of ABC transporters in plants. Essays Biochem. 50, 145–160. https://doi.org/10.1042/bse0500145.
Laakso, T.A., Sperling, E.A., Johnston, D.T., Knoll, A.H., 2020. Ediacaran reorganization of the marine phosphorus cycle. Proc. Natl. Acad. Sci. 117, 11961–11967. https://doi.org/10.1073/pnas.1916738117.
Ladds, G., Davey, J., 2000. Identification of proteases with shared functions to the proprotein processing protease Krp1 in the fission yeast *Schizosaccharomyces pombe*. Mol. Microbiol. 38, 839–853. https://doi.org/10.1046/j.1365-2958.2000.02180.x.
Leal, J.F., Cristiano, M.L.S., 2022. Marine paralytic shellfish toxins: chemical properties, mode of action, newer analogues, and structure–toxicity relationship. Nat. Prod. Rep. 39, 33–57. https://doi.org/10.1039/d1np00009h.
Leterrier, M., Barroso, J.B., Valderrama, R., Begara-Morales, J.C., Sánchez-Calvo, B., Chaki, M., Luque, F., Viñegla, B., Palma, J.M., Corpas, F.J., 2016. Peroxisomal NADP-isocitrate dehydrogenase is required for *Arabidopsis* stomatal movement. Protoplasma 253, 403–415. https://doi.org/10.1007/s00709-015-0819-0.
Levin, E., Kishore, A., Ballester, A.R., Raphael, G., Feigenberg, O., Liu, Y., Norelli, J., Gonzalez-Candelas, L., Wisniewski, M., Droby, S., 2019. Identification of pathogenicity-related genes and the role of a subtilisin-related peptidase S8 (PePRT) in authophagy and virulence of *Penicillium expansum* on apples. Postharvest Biol. Technol. 149, 209–220. https://doi.org/10.1016/j.postharvbio.2018.10.011.
Li, D.W., Tan, J.Z., Li, Z.F., Ou, L.J., 2024. Membrane lipid remodeling and autophagy to cope with phosphorus deficiency in the dinoflagellate *Prorocentrum shikokuense*. Chemosphere 349, 140844. https://doi.org/10.1016/j.chemosphere.2023.140844.
Lilly, E.L., 2002. Paralytic shellfish poisoning toxins in France linked to a human-introduced strain of *Alexandrium catenella* from the western Pacific: evidence from DNA and toxin analysis. J. Plankton Res. 24, 443–452. https://doi.org/10.1093/plankt/24.5.443.
Lin, S., Cheng, S., Song, B., Zhong, X., Lin, X., Li, W., Li, L., Zhang, Y., Zhang, H., Ji, Z., Cai, M., Zhuang, Y., Shi, X., Lin, L., Wang, L., Wang, Z., Liu, X., Yu, S., Zeng, P., Hao, H., Zou, Q., Chen, C., Li, Y., Wang, Y., Xu, C., Meng, S., Xu, X., Wang, J., Yang, H., Campbell, D.A., Sturm, N.R., Dagenais-Bellefeuille, S., Morse, D., 2015. The *Symbiodinium kawagutii* genome illuminates dinoflagellate gene expression and coral symbiosis. Science 350, 691–694. https://doi.org/10.1126/science.aad0408.
Lin, S., Litaker, R.W., Sunda, W.G., 2016. Phosphorus physiological ecology and molecular mechanisms in marine phytoplankton. J. Phycol. 52, 10–36. https://doi.org/10.1111/jpy.12365.
Lin, X., Zhang, H., Cui, Y., Lin, S., 2012a. High sequence variability, diverse subcellular localizations, and ecological implications of alkaline phosphatase in dinoflagellates and other eukaryotic phytoplankton. Front. Microbiol. 3, 235. https://doi.org/10.3389/fmicb.2012.00235.
Lin, X., Zhang, H., Huang, B., Lin, S., 2012b. Alkaline phosphatase gene sequence characteristics and transcriptional regulation by phosphate limitation in *Karenia brevis* (Dinophyceae). Harmful Algae 17, 14–24. https://doi.org/10.1016/j.hal.2012.02.005.
Luo, H., Lin, X., Li, L., Lin, L., Zhang, C., Lin, S., 2017. Transcriptomic and physiological analyses of the dinoflagellate *Karenia mikimotoi* reveal non-alkaline phosphatase-based molecular machinery of ATP utilisation. Environ. Microbiol. 19, 4506–4518. https://doi.org/10.1111/1462-2920.13899.
Makowka, A., Nichelmann, L., Schulze, D., Spengler, K., Wittmann, C., Forchhammer, K., Gutekunst, K., 2020. Glycolytic shunts replenish the Calvin–Benson–Bassham cycle as anaplerotic reactions in cyanobacteria. Mol. Plant 13, 471–482. https://doi.org/10.1016/j.molp.2020.02.002.
Mitra, K., Frank, J., Driessen, A., 2006. Co- and post-translational translocation through the protein-conducting channel: analogous mechanisms at work? Nat. Struct. Mol. Biol. 13, 957–964. https://doi.org/10.1038/nsmb1166.
Mitra, K., Ubarretxena-Belandia, I., Taguchi, T., Warren, G., Engelman, D.M., 2004. Modulation of the bilayer thickness of exocytic pathway membranes by membrane proteins rather than cholesterol. Proc. Natl. Acad. Sci. 101, 4083–4088. https://doi.org/10.1073/pnas.0307332101.
Mix, A.K., Cenci, U., Heimerl, T., Marter, P., Wirkner, M.L., Moog, D., 2018. Identification and localization of peroxisomal biogenesis proteins indicates the presence of peroxisomes in the cryptophyte *Guillardia theta* and other "chromalveolates". Genome Biol. Evol. 10, 2834–2852. https://doi.org/10.1093/gbe/evy214.
Moosavi, B., Berry, E.A., Zhu, X.L., Yang, W.C., Yang, G.F., 2019. The assembly of succinate dehydrogenase: a key enzyme in bioenergetics. Cell. Mol. Life Sci. 76, 4023–4042. https://doi.org/10.1007/s00018-019-03200-7.
Mullins, C., Meyer, H.A., Hartmann, E., Green, N., Fang, H., 1996. Structurally related Spc1p and Spc2p of yeast signal peptidase complex are functionally distinct. J. Biol. Chem. 271, 29094–29099. https://doi.org/10.1074/jbc.271.46.29094.
Nawrocki, M.P., Karl, D.M., 1989. Dissolved ATP turnover in the Bransfield Strait, Antarctica during a spring bloom. Mar. Ecol. Prog. Ser. 57, 35–44. https://doi.org/10.3354/meps057035.
Nelson, W.J., Yeaman, C., 2001. Protein trafficking in the exocytic pathway of polarized epithelial cells. Trends Cell Biol. 11, 483–486. https://doi.org/10.1016/s0962-8924(01)02145-6.
Orchard, E.D., Webb, E.A., Dyhrman, S.T., 2009. Molecular analysis of the phosphorus starvation response in *Trichodesmium* spp. Environ. Microbiol. 11, 2400–2411. https://doi.org/10.1111/j.1462-2920.2009.01968.x.
Paerl, H.W., Hall, N.S., Calandrino, E.S., 2011. Controlling harmful cyanobacterial blooms in a world experiencing anthropogenic and climatic-induced change. Sci. Total Environ. 409, 1739–1745. https://doi.org/10.1016/j.scitotenv.2011.02.001.
Paerl, H.W., Otten, T.G., 2013. Harmful cyanobacterial blooms: causes, consequences, and controls. Microb. Ecol. 65, 995–1010. https://doi.org/10.1007/s00248-012-0159-y.
Parsons, T.R., Maita, Y., Lalli, C.M., 1984. A Manual of Chemical and Biological Methods for Seawater Analysis. Pergamon Press, New York, USA. https://doi.org/10.1016/C2009-0-07774-5.
Pearson, L.A., Hisbergues, M., Borner, T., Dittmann, E., Neilan, B.A., 2004. Inactivation of an ABC transporter gene, *mcyH*, results in loss of microcystin production in the cyanobacterium *Microcystis aeruginosa* PCC 7806. Appl. Environ. Microbiol. 70, 6370–6378. https://doi.org/10.1128/AEM.70.11.6370-6378.2004.
Penna, A., Garcés, E., Vila, M., Giacobbe, M.G., Fraga, S., Lugliè, A., Bravo, I., Bertozzini, E., Vernesi, C., 2005. *Alexandrium catenella* (Dinophyceae), a toxic ribotype expanding in the NW Mediterranean Sea. Mar. Biol. 148, 13–23. https://doi.org/10.1007/s00227-005-0067-5.
Poirier, Y., Bucher, M., 2002. Phosphate transport and homeostasis in arabidopsis. Arabidopsis Book 1, e0024. https://doi.org/10.1199/tab.0024.
Raden, D., Song, W., Gilmore, R., 2000. Role of the cytoplasmic segments of Sec61α in the ribosome-binding and translocation-promoting activities of the sec61 complex. J. Cell Biol. 150, 53–64. https://doi.org/10.1083/jcb.150.1.53.
Ralph, P.J., Gademann, R., 2005. Rapid light curves: a powerful tool to assess photosynthetic activity. Aquat. Bot. 82, 222–237. https://doi.org/10.1016/j.aquabot.2005.02.006.
Ren, L., Wang, P., Wang, C., Chen, J., Hou, J., Qian, J., 2017. Algal growth and utilization of phosphorus studied by combined mono-culture and co-culture experiments. Environ. Pollut. 220, 274–285. https://doi.org/10.1016/j.envpol.2016.09.061.
Roy, S., Letourneau, L., Morse, D., 2014. Cold-induced cysts of the photosynthetic dinoflagellate *Lingulodinium polyedrum* have an arrested circadian bioluminescence rhythm and lower levels of protein phosphorylation. Plant Physiol. 164, 966–977. https://doi.org/10.1104/pp.113.229856.
Rumpho, M.E., Pochareddy, S., Worful, J.M., Summer, E.J., Bhattacharya, D., Pelletreau, K.N., Tyler, M.S., Lee, J., Manhart, J.R., Soule, K.M., 2009. Molecular characterization of the Calvin cycle enzyme phosphoribulokinase in the stramenopile alga *Vaucheria litorea* and the plastid hosting mollusc *elysia chlorotica*. Mol. Plant 2, 1384–1396. https://doi.org/10.1093/mp/ssp085.
Sandalio, L.M., Romero-Puertas, M.C., 2015. Peroxisomes sense and respond to environmental cues by regulating ROS and RNS signalling networks. Ann. Bot-London. 116, 475–485. https://doi.org/10.1093/aob/mcv074.
Schindler, D.W., Hecky, R.E., Findlay, D.L., Stainton, M.P., Parker, B.R., Paterson, M.J., Beaty, K.G., Lyng, M., Kasian, S.E.M., 2008. Eutrophication of lakes cannot be controlled by reducing nitrogen input: results of a 37-year whole-ecosystem experiment. Proc. Natl. Acad. Sci. 105, 11254–11258. https://doi.org/10.1073/pnas.0805108105.
Shahin, L., Zhang, L., Mohnen, D., Urbanowicz, B.R., 2023. Insights into pectin O-acetylation in the plant cell wall: structure, synthesis, and modification. The Cell Surface 9, 100099. https://doi.org/10.1016/j.tcsw.2023.100099.
Sharwood, R.E., Sonawane, B.V., Ghannoum, O., Whitney, S.M., 2016. Improved analysis of C4 and C3 photosynthesis via refined in vitro assays of their carbon fixation biochemistry. J. Exp. Bot. 67, 3137–3148. https://doi.org/10.1093/jxb/erw154.
Smayda, T.J., 2001. Community assembly in marine phytoplankton: application of recent models to harmful dinoflagellate blooms. J. Plankton Res. 23, 447–461. https://doi.org/10.1093/plankt/23.5.447.
Sommer, J.R., Blum, J.J., 1965. Cytochemical localization of acid phosphatases in *Euglena gracilis*. J. Cell Biol. 24, 235–251. https://doi.org/10.1083/jcb.24.2.235.
Sopory, S.K., Munshi, M., 1998. Protein kinases and phosphatases and their role in cellular signaling in plants. Crit. Rev. Plant Sci. 17, 245–318. https://doi.org/10.1080/07352689891304230.
Svensson, S., Särngren, A., Förlin, L., 2003. Mussel blood cells, resistant to the cytotoxic effects of okadaic acid, do not express cell membrane p-glycoprotein activity (multixenobiotic resistance). Aquat. Toxicol. 65, 27–37. https://doi.org/10.1016/s0166-445x(03)00097-3.
Thingstad, T.F., Krom, M.D., Mantoura, R.F.C., Flaten, G.A.F., Groom, S., Herut, B., Kress, N., Law, C.S., Pasternak, A., Pitta, P., Psarra, S., Rassoulzadegan, F., Tanaka, T., Tselepides, A., Wassmann, P., Woodward, E.M.S., Riser, C.W., Zodiatis, G., Zohary, T., 2005. Nature of phosphorus limitation in the ultraoligotrophic eastern Mediterranean. Science 309, 1068–1071. https://doi.org/10.1126/science.1112632.
Tyrrell, T., 1999. The relative influences of nitrogen and phosphorus on oceanic primary production. Nature 400, 525–531. https://doi.org/10.1038/22941.
Van Mooy, B.A.S., Fredricks, H.F., Pedler, B.E., Dyhrman, S.T., Karl, D.M., Koblížek, M., Lomas, M.W., Mincer, T.J., Moore, L.R., Moutin, T., Rappé, M.S., Webb, E.A., 2009. Phytoplankton in the ocean use non-phosphorus lipids in response to phosphorus scarcity. Nature 458, 69–72. https://doi.org/10.1038/nature07659.
Vaulot, D., Lebot, N., Marie, D., Fukai, E., 1996. Effect of phosphorus on the synechococcus cell cycle in surface Mediterranean waters during summer. Appl. Environ. Microbiol. 62, 2527–2533. https://doi.org/10.1128/aem.62.7.2527-2533.1996.
Wang, B., Yang, J., Xu, C., Yi, L., Wan, C., 2020. Dynamic expression of intra- and extracellular proteome and the influence of epiphytic bacteria for *Nostoc flagelliforme* in response to rehydration. Environ. Microbiol. 22, 1251–1264. https://doi.org/10.1111/1462-2920.14931.

Wang, D.Z., Zhang, H., Zhang, Y., Zhang, S.F., 2014. Marine dinoflagellate proteomics: current status and future perspectives. J. Proteonomics 105, 121–132. https://doi.org/10.1016/j.jprot.2014.01.026.

Wang, H., Kim, H., Park, H., Ki, J.S., 2022. Temperature influences the content and biosynthesis gene expression of saxitoxins (STXs) in the toxigenic dinoflagellate *Alexandrium pacificum*. Sci. Total Environ. 802, 149801. https://doi.org/10.1016/j.scitotenv.2021.149801.

Wang, Z., Liang, Y., Kang, W., 2011. Utilization of dissolved organic phosphorus by different groups of phytoplankton taxa. Harmful Algae 12, 113–118. https://doi.org/10.1016/j.hal.2011.09.005.

Will, C.L., Luhrmann, R., 2011. Spliceosome structure and function. Csh. Perspect. Biol. 3, a003707. https://doi.org/10.1101/cshperspect.a003707.

Wu, N., Ma, Y.C., Gong, X.Q., Zhao, P.J., Jia, Y.J., Zhao, Q., Duan, J.H., Zou, C.G., 2023. The metabolite alpha-ketobutyrate extends lifespan by promoting peroxisomal function in *C. elegans*. Nat. Commun. 14, 240. https://doi.org/10.1038/s41467-023-35899-1.

Wu, T., Fu, Y., Shi, Y., Li, Y., Kou, Y., Mao, X., Liu, J., 2020. Functional characterization of long-chain Acyl-CoA synthetase gene family from the oleaginous alga *Chromochloris zofingiensis*. J. Agric. Food Chem. 68, 4473–4484. https://doi.org/10.1021/acs.jafc.0c01284.

Wurch, L.L., Bertrand, E.M., Saito, M.A., Van Mooy, B.A.S., Dyhrman, S.T., 2011. Proteome changes driven by phosphorus deficiency and recovery in the brown tide-forming alga *Aureococcus anophagefferens*. PLoS One 6, e28949. https://doi.org/10.1371/journal.pone.0028949.

Wyatt, T., Jenkinson, I.R., 1997. Notes on *Alexandrium* population dynamics. J. Plankton Res. 19, 551–575. https://doi.org/10.1093/plankt/19.5.551.

Xu, L., Lin, R., Li, X., Zhang, C., Yang, X., Guo, L., Yu, H., Gao, X., Hu, C., 2023. Comparative proteomic analyses within three developmental stages of the mushroom white *Hypsizygus marmoreus*. J. Fungi 9, 225. https://doi.org/10.3390/jof9020225.

Yang, Y., Shi, J., Jia, Y., Bai, F., Yang, S., Mi, W., He, S., Wu, Z., 2020. Unveiling the impact of glycerol phosphate (DOP) in the dinoflagellate *Peridinium bipes* by physiological and transcriptomic analysis. Environ. Sci. Eur. 32, 38. https://doi.org/10.1186/s12302-020-00317-6.

Yegorov, Y., Sendersky, E., Zilberman, S., Nagar, E., Waldman Ben-Asher, H., Shimoni, E., Simkovsky, R., Golden, S.S., LiWang, A., Schwarz, R., 2021. A cyanobacterial component required for pilus biogenesis affects the exoproteome. mBio 12, e03674. https://doi.org/10.1128/mBio.03674-20, 20.

Yu, R., Zhang, Q., Kong, F., Zhou, Z., Chen, Z., Zhao, Y., Geng, H., Dai, L., Yan, T., Zhou, M., 2017. Status, impacts and long-term changes of harmful algal blooms in the sea area adjacent to the Changjiang River estuary. Oceanol. Limnol. Sinica 48, 1178–1186. https://doi.org/10.11693/hyhz20170900247.

Zhang, C., Lin, S., Huang, L., Lu, W., Li, M., Liu, S., 2014. Suppression subtraction hybridization analysis revealed regulation of some cell cycle and toxin genes in *Alexandrium catenella* by phosphate limitation. Harmful Algae 39, 26–39. https://doi.org/10.1016/j.hal.2014.06.005.

Zhang, Q., Chen, Y., Wang, M., Zhang, J., Chen, Q., Liu, D., 2021. Molecular responses to inorganic and organic phosphorus sources in the growth and toxin formation of *Microcystis aeruginosa*. Water Res. 196, 117048. https://doi.org/10.1016/j.watres.2021.117048.

Zhang, Q., Song, Q., Wang, C., Zhou, C., Lu, C., Zhao, M., 2017. Effects of glufosinate on the growth of and microcystin production by *Microcystis aeruginosa* at environmentally relevant concentrations. Sci. Total Environ. 575, 513–518. https://doi.org/10.1016/j.scitotenv.2016.09.011.

Zhang, S., Chen, Y., Xie, Z., Zhang, H., Lin, L., Wang, D., 2019a. Unraveling the molecular mechanism of the response to changing ambient phosphorus in the dinoflagellate *Alexandrium catenella* with quantitative proteomics. J. Proteonomics 196, 141–149. https://doi.org/10.1016/j.jprot.2018.11.004.

Zhang, S., Yuan, C., Chen, Y., Lin, L., Wang, D., 2019b. Transcriptomic response to changing ambient phosphorus in the marine dinoflagellate *Prorocentrum donghaiense*. Sci. Total Environ. 692, 1037–1047. https://doi.org/10.1016/j.scitotenv.2019.07.291.

Zhao, S., Li, X., Yao, X., Wan, W., Xu, L., Guo, L., Bai, J., Hu, C., Yu, H., 2024. Transformation of antibiotics to non-toxic and non-bactericidal products by laccases ensure the safety of *Stropharia rugosoannulata*. J. Hazard Mater. 476, 135099. https://doi.org/10.1016/j.jhazmat.2024.135099.

Zhou, M., Shen, Z., Yu, R., 2008. Responses of a coastal phytoplankton community to increased nutrient input from the Changjiang (Yangtze) River. Cont. Shelf. Res. 28, 1483–1489. https://doi.org/10.1016/j.csr.2007.02.009.